Ameera J. Kadhm
Israa A. Abbas

Department of Physics, College of Education for Pure Sciences, Al-Mustansiriyah University, Baghdad, IRAQ

Optical properties of PVA Doped with CGNS Nanosheets

The PVA polymers doped with coarse-grained graphene nanosheets (CGNS) with different concentrations (3, 6, and 9 wt.%) were prepared by the pulsed laser ablation technique. The Fourier-transform infrared (FTIR) spectroscopy, optical microscopy, x-ray diffraction (XRD), and UV-visible spectrophotometry were used to study the structural and optical characteristics of the prepared PVA-CGNS nanocomposites. When the concentration of CGNS is increased, the absorbance, index of refraction, and imaginary and real dielectric constants increased while the transmittance and energy band gap decreased. The allowed indirect energy gap decreased from 4.54 to 4.257 eV and the forbidden indirect energy gap decreased from 3.79 to 2.89 eV. The results are encouraging to use this nanocomposite for radiation shielding, spectroscopic devices, and other applications.

Keywords: Laser ablation; CGNS; Optical energy gap; Nanocomposites
Received: 02 September 2023; **Revised:** 01 October 2023; **Accepted:** 08 October 2023

1. Introduction

Nanotechnology research & development is now prioritized as one of the most active topics in almost all technological fields [1,2]. Polymer nanocomposites need to get more attention since they are more effective. This explains how the nanofillers affect the mechanical, structural, and other properties. However, the nanofillers are lighter and require fewer reinforcements than other matrix components [3]. As a result, several research have centered on designing and simulating various components to improve the mechanical properties of various nanocomposite materials [4,5]. Abdullah et al. [6] used a simple solution approach was used to create a PVA/Graphene nanocomposite. As the amount of graphene in the sample increased, the transparency of the nanocomposite samples decreased. Pei et al. [7] improved the mechanical and physical properties to get over the drawbacks of existing modification techniques utilizing polymer and nanomaterials, graphene and polyvinyl alcohol (PVA) were mixed in a single process to modify a composite cementitious material. Li et al. [8] used a proprietary continuous needle-free a dynamic linear electro-spinning method for manufacturing large-scale nanostructures composed of carbon-nanotubes (CNT), graphene (Gr), polyvinyl alcohol (PVA), and sodium alginate (SA) produced nanofiber membranes. Cobos et al. [9] used ascorbic acid (L-AA) to in-situ reduce graphene oxide (GO) dispersed in a PVA solution to obtain a polymer filled with uniformly dispersed graphene (GS) sheets. The fabrication of (vinyl alcohol) (PVA)-based nanocomposite films is described as an environmentally friendly reducing agent. They argued the moisture barrier is improved by GS and nanocomposite films' resilience to water via decreasing PVA's water absorption and water vapor permeability [10]. The PVA polymer was selected for this study due to a number of factors, including its safety and chemical inertness. Various image and non-imaging microelectronics and sensors can be used with it, according to previous statements [11]. PVA is frequently combined with other polymer substances, including bio-polymers and other hydrophilic polymers. Improvements are made to the chemical, structural, and physical properties of the polymeric matrix by the inclusion of an inorganic material [12]. Carbon hexagons are arranged in a single layer to form graphene, which also contains electron clouds and C-C bonds that have undergone sp^2 hybridization. Because of their intriguing structure, unique physical characteristics, and potential future uses in technical fields, thin flakes consisting of several layers of carbon atoms, such as single-layer graphene, can be extremely important in engineering [13]. Kadhm and Abbas [14] have prepared pure zinc and coordinated copper nanomembranes and coatings on NiO with different concentrations (1, 3, 5%) at a temperature of 298 K, and their combination at 5% were formed on a glass substrate by a sol-gel process. Optical properties of Zn doped NiO, Cu, and nano NiO were investigated over the wavelength range of 300-800 nm, with increased transmittance value of 94% in visible-NIR region [15]. The production of poly(vinylalcohol) (PVA) with different RGO loading ratios (1, 1.5, 2 wt.%) was described. The nanocomposites were prepared using a solution mixing process and an evaporative casting approach. The impact of frequency in the 100 Hz to 1.5 MHz range on temperature-dependent dielectric characteristics was the main subject of this investigation.

The goal of this work is to use pulsed laser ablation technique to prepare thin film PVA-CGNS nanocomposites with varied concentrations of (CGNS) nanosheets. The produced nanocomposites are next characterized and studied in terms of structural and optical characteristics.

2. Material and Methods

The graphite powder of 5g and purity of 99.98% supplied by Interchimiques SA from France was sued. After using ethanol to clean it, a hydraulic piston was used to compress the cylinder at a pressure of 20 MPa, 2 cm wide, 2 mm thick, and then strengthened by annealing at temperature of 450°C for 4 hours. A graphite plate was cleaned with fresh paper, then rinsed with ethanol and distilled water to eliminate the debasements. A 0.5g of PVA (density of 1.18 g/cm^3, glass temperature of 75°C, and molecular weight of 18000 g/mol) has been heated to 50°C using a magnetic stirrer in 30 ml of distilled water for 30 minutes. The produced graphite plate was inserted into a glass jar with 5 ml of PVA solution buried 2 mm below the liquid surface on a bracket. Then, a Q-switched Nd:YAG laser with pulse duration of 10 ns, repetition rate of 6 Hz, and peak energy of 80 mJ at wavelength of 1064 nm was sued. The number of pulses was 300. The optical properties of the colloid were determined using a Shimadzu 1800 UV-Visible-NIR spectrophotometer in the spectral range of 200-1100nm. Scanning electron microscopy (SEM) and Fourier-transform infrared (FTIR) spectroscopy were used to introduce the morphology and structural characteristics of the prepared samples. The samples were prepared as thin films on a silicon wafer using the spin coating process for 20 s at a speed of 500 rpm.

3. Results and Discussion

The results and discussion of the structural and optical measurements for PVA-CGNS nanocomposites are presented herein. The effect of varying concentration of additive nanoparticles (CGNS) was studied by the optical microscopy.

Figure (1) shows optical microscope images (40X magnification) of PVA and PVA-CGNS nanocomposites with varying CGNS concentrations. These images demonstrated the excellent homogeneity of the matrix and good dispersion of graphene into the PVA polymer. They revealed that the PVA-CGNS nanocomposites were successfully synthesized utilizing this approach. In compared to polymer (PVA) films, PVA-CGNS nanocomposites films showed a significant alteration when the CGNS concentrations was increased.

The optical properties of PVA-CGNS nanocomposites can be studied to identify the impact of adding CGNS nanoparticles on the optical properties of PVA polymer. The types of electronic transitions are also described in this section, along with methods for calculating energy gaps, absorption coefficients, extinction coefficients, and other optical constants.

The absorption spectra of a nanocomposite (PVA-CGNS) are shown in Fig. (2) as a function of the wavelength of incident light. These spectra demonstrate that the absorbance of all films is maximum around the fundamental absorption edge (310nm), then decreases in the visible and NIR regions. The absorption of the film is typically decreasing with increasing wavelength. This phenomenon can be explained as follows. The photon will transmit when incident photons lack the energy to interact with atoms at long wavelengths. As the wavelength is decreased and the absorbance increases, the incident photons will interact with the material [16,17].

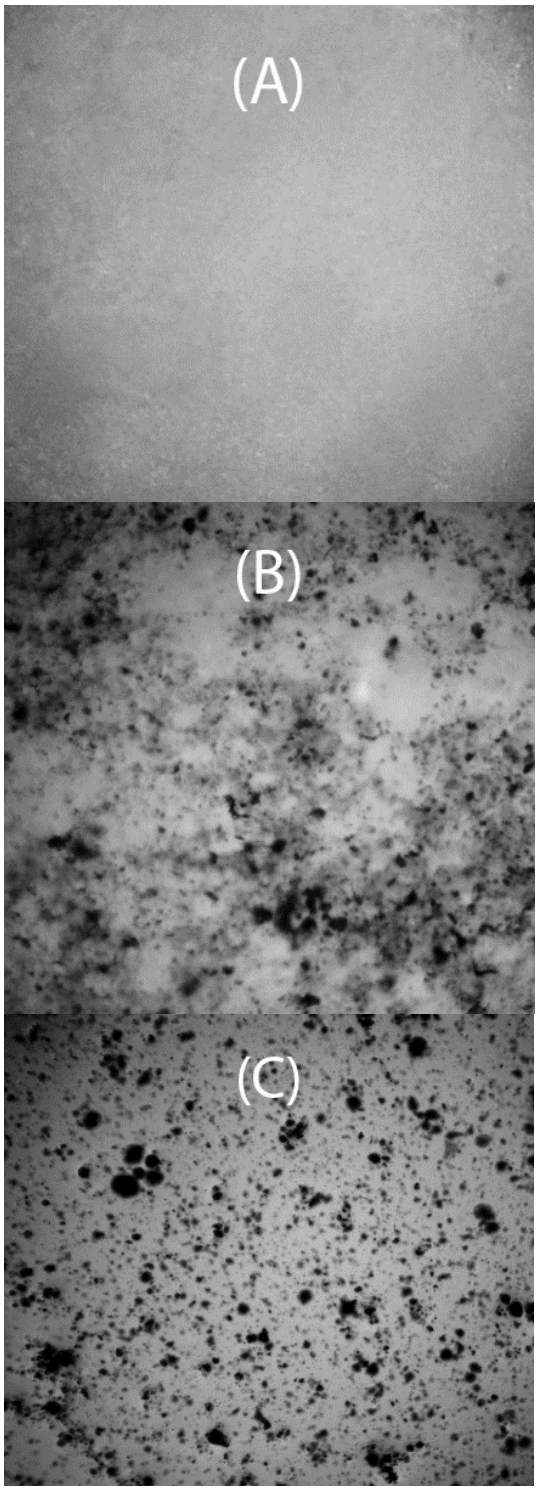

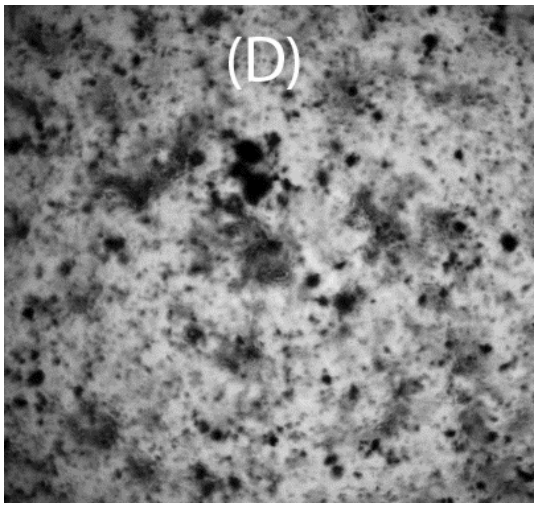

Fig. (1) Microscope images (40X) for PVA polymer and PVA-CGNS nanocomposites: (A) for PVA, (B) for 3wt.% CGNS, (C) for 6wt.% CGNS, (D) for 9wt.% CGNS

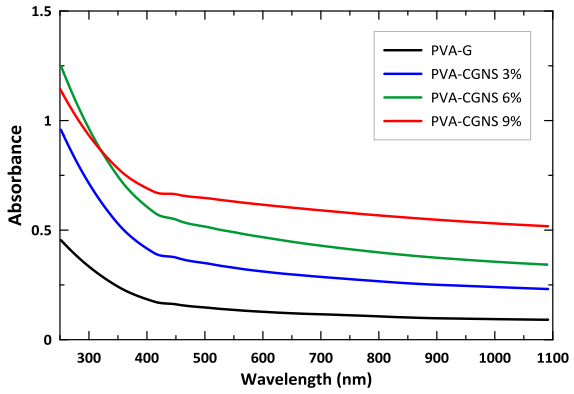

Fig. (2) Absorption spectra of PVA polymer and PVA-CGNS nanocomposite as a function of wavelength

The transmission spectra of the PVA polymer and PVA-CGNS nanocomposites are shown in Fig. (3). These spectra depict the total sample transmittance at about 240 nm, the increase becomes approximately constant, and beyond 260 nm, the increase becomes almost constant. The results clearly show that the CGNS cause to decrease the transmittance. The CGNS contribution ratio in the matrix was increased to improve this behavior, where the increase in nanomaterial amount (concentration) might increase light absorption and decrease transmission for the same reason. At 600nm, the results showed a 9%, 17%, and 21% decrease in transmittance with increasing the CGNS ratio to 3, 6, and 9%, respectively.

In order to determine the energy gap (E_g) of the prepared samples, Tauc's relation is used as [18]:

$$\alpha h\nu = B\left[h\nu - E_g\right]^r \quad (1)$$

Here α is the absorption coefficient determined from the absorbance, B is a constant, $h\nu$ is the photon energy, r=2 for allowed indirect transitions and r=3 for forbidden indirect transitions

Figure (4) depicts the absorption coefficients of PVA polymer and PVA-CGNS nanocomposite films as a function of photon energy. The behavior of absorption coefficient indicated a constant increase with increasing photon energy up to 4.7eV. This might be related to the electron's lower transition, where the input photon energy was insufficient to transfer an electron from the valence band to the conduction band. In contrast, the coefficient of absorption beyond 4.7eV shows a sharp increase in all sample because of the strong transitions of electrons to the conduction band. The results revealed that increasing the concentration of CGNS in the nanocomposites up to 3, 6, and 9% improved the absorption coefficient at 4.5eV by about 106, 205, and 445%, respectively.

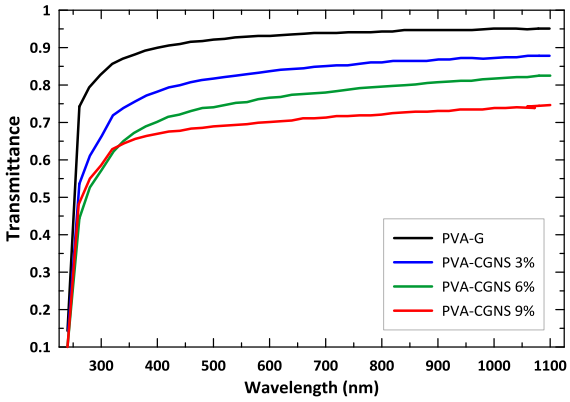

Fig. (3) Transmission spectra of PVA polymer and PVA-CGNS nanocomposite as a function of wavelength

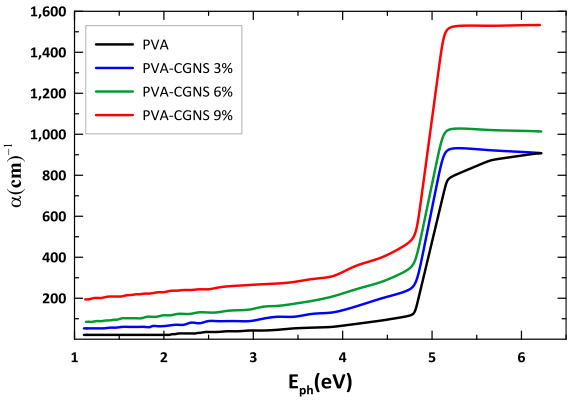

Fig. (4) Variation of absorption coefficient (α) for PVA blend and PVA-CGNS nanocomposite with photon energy

The following equation was used to determine the index of refraction (n) for PVA and PVA-CGNS blends:

$$n = \left[1 + R^{\frac{1}{2}}\right]\left[1 - R^{\frac{1}{2}}\right] \quad (2)$$

Figure (5) shows the relationship between the absorption edge $(\alpha h\nu)^{1/2}$ with photon energy (E_{ph}) for allowed indirect transition as the linear part of the curve is extrapolated to intersect the x-axis to determine the value of optical energy gap as $(\alpha h\nu)^{1/2}=0$.

Figure (6) shows the relationship between the absorption edge $(\alpha h\nu)^{1/3}$ and photon energy for PVA-

CGNS nanocomposites. The optical energy gap clearly decreases as the weight percentage of polydopamine nanoparticles is increased. This is due to the formation of inter-band levels within the optical energy gap [19]. Hence, the transition occurs in two phases in this situation, as a result of increasing the weight percentage of CGNS nanoparticles, the conduction band receives electrons that have moved from the local levels of the valence band.

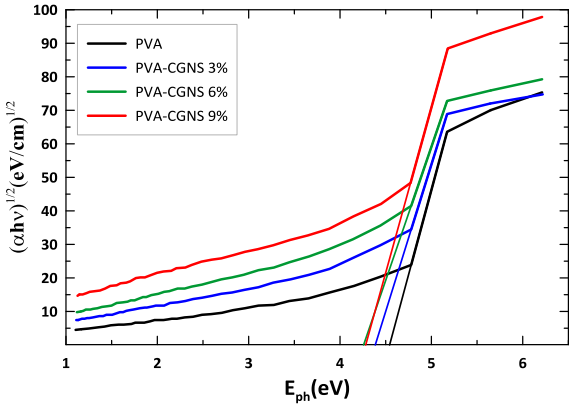

Fig. (5) Variation of $(\alpha h\upsilon)^{1/2}$ with photon energy for PVA blend and PVA-CGNS nanocomposites

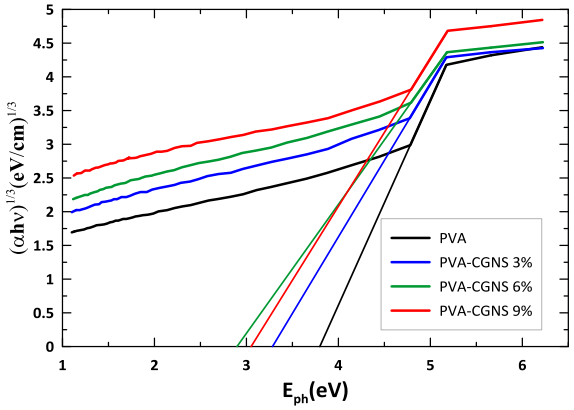

Fig. (6) Variation of $(\alpha h\upsilon)^{1/3}$ with photon energy for PVA blend and PVA-CGNS nanocomposites

The two parts (real ε_1 and imaginary ε_2) of the dielectric constant (ε) are calculated using the following equations:

$$\varepsilon_1 = (n^2 - k^2) \quad (3)$$

$$\varepsilon_2 = 2nk \quad (4)$$

Figure (7) depicts the extinction coefficient (K) of the PVA and PVA-CGNS nanocomposite films as a function of wavelength. The extinction coefficient of nanocomposites was higher in the UV region. This characteristic was caused by high absorbance of all nanocomposites. The same behavior is observed in the visible-NIR regions. These findings showed that the addition of CGNS nanosheets significantly improved the behavior of the nanocomposites, especially at higher ratios of the CGNS employed in this study, which showed an overall improvement in the outcomes when compared to other nanocomposites [20] as well as with increasing wavelength, as clearly shown in Fig. (7). The results indicated that increasing the weight percentage of graphene oxide in the nanocomposites by 3, 6, and 9% led to considerable improvements in extinction coefficients of up to 49%, 317%, and 715% at 600nm.

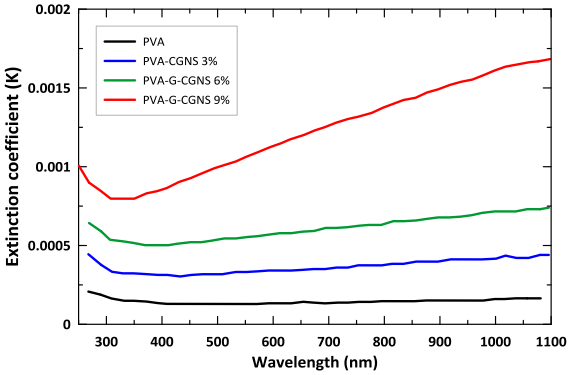

Fig. (7) Extinction coefficient as a function of wavelength for PMMA-PVA blend and PMMA-PVA/PDA nanocomposites

The variation of index of refraction with wavelength for PVA and PVA-CGNS nanocomposites are depicted in Fig. (8). The index of refraction of nanocomposites increased as a result of the addition of GO nanosheets. This behavior may be explained by making nanocomposites denser. The results revealed that adding GO to the nanocomposite at concentrations of 3, 6, and 9% led to substantial improvements in the index of refraction up to 22%, 36%, and 49% at 600nm.

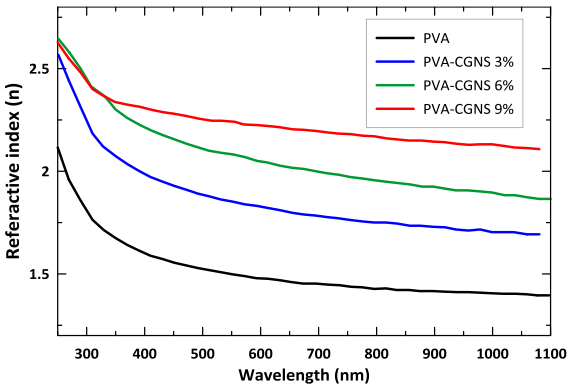

Fig. (8) Variation of the index of refraction with the wavelength for PVA blend and PVA-CGNS nanocomposites

The imaginary and real parts of the dielectric constant of PVA and PVA-CGNS nanocomposite films vary with wavelength, as seen in figures (9) and (10). These data demonstrate that the real and imaginary dielectric constants were enhanced as the concentration of CGNS nanosheets was increased. This occurs as a result of the increase in electrical polarization of the nanocomposites. The findings indicated that increasing the concentrations of CGNS by 3%, 6%, and 9% in the nanocomposite at 600nm will increase the values of real and imaginary

dielectric constants for by 23%, 69%, 203% and 51%, 89%, 119%, respectively.

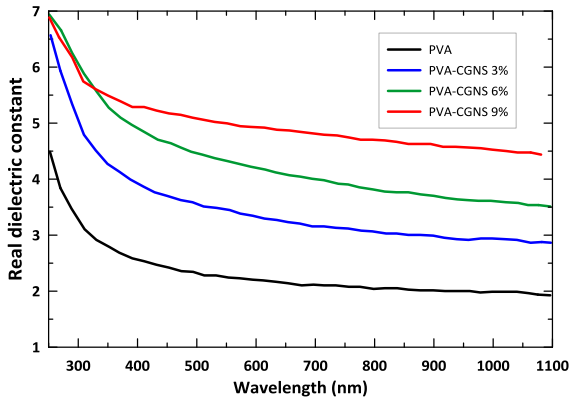

Fig. (9) Variation of real part of dielectric constant for PVA blend and PVA-CGNS nanocomposites with wavelength

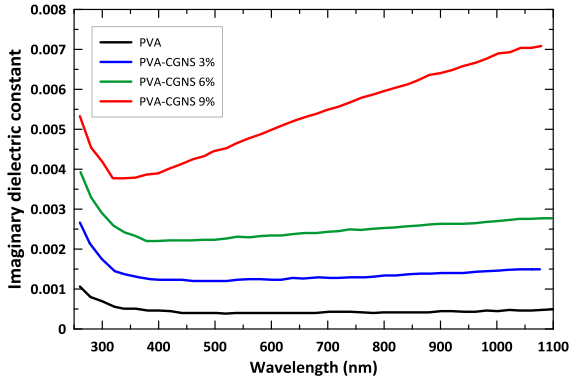

Fig. (10) Variation of the imaginary component of the dielectric constant for PVA blend and PVA-CGNS nanocomposites with wavelength

4. Conclusion

The PVA-CGNS nanocomposite was prepared by pulsed laser ablation technique with different concentrations of CGNS nanosheets (3, 6 and 9 wt.%). The absorption of UV light was increased with increasing the concentration of GGNS nanosheets in the nanocomposite, which makes these films suitable for several applications, for instance as low-cost UV protection, solar radiation shields, industry of sunglasses to protect the human eye, and as packaging for energy storage. Fundamental absorption edge and optical band gap for both allowed and forbidden indirect transition showed decrease with increasing GGNS weight percentage.

References

[1] D.R. Paul and L.M. Robeson, "Polymer Nanotechnology: Nanocomposites", *Polymer*, 49 (2008) 3187-3204.

[2] B. Bhushan (editor), "**Springer Handbook of Nanotechnology"**, Springer, Ch. 2, p. 32.

[3] R.V. Kurahatti et al., "Applications of Polymer Nanocomposites", *Def. Sci. J.*, 60 (2010) 555-563.

[4] Y.-W. Mai, and Y. Zhong-Zhen. "**Polymer Nanocomposites**", Woodhead Pub. Ltd. (2006), Ch. 3, p. 23.

[5] F. Deng et al., "Effects of anisotropy, aspect ratio, and no straightness of carbon nanotubes on thermal conductivity of carbon nanotube composites", *Appl. Phys. Lett.*, 90(2) (2007) 21914.

[6] A.H. Abdullah et al., "PVA/Graphene nanocomposite: morphology and its thermal properties", *IOP Conf. Ser.: Mater. Sci. Eng.*, 319(1) (2018) 012011.

[7] C. Pei et al., "Synergistic effects of a novel method of preparing graphene/polyvinyl alcohol to modify cementitious material", *Construct. Build. Mater.*, 258 (2020) 119647.

[8] T.T. Li et al., "Synergistic effect and characterization of graphene/carbon nanotubes/polyvinyl alcohol/sodium alginate nanofibrous membranes formed using continuous needleless dynamic linear electrospinning", *Nanomaterials*, 9(5) (2019) 714.

[9] M. Cobos, M.J. Fernández and M.D. Fernández, "Graphene based poly(Vinylalcohol) nanocomposites prepared by *in situ* green reduction of graphene oxide by ascorbic acid: Influence of graphene content and glycerol plasticizer on properties", *Nanomaterials*, 8(12) (2018) 1013.

[10] L. Huang et al., "Recent progress and applications of cellulose and its derivatives-based humidity sensors: A review", *Carbohyd. Polym.*, 318 (2023) 121139.

[11] R. Belluomo, A. Khodaei and S.A. Yavari, "Additively manufactured Bi-functionalized bioceramics for reconstruction of bone tumor defects", *Acta Biomaterialia*, 156 (2023) 234-249.

[12] M. Cui, S.J. Park and S. Kim, "Carboxylated group effect of graphene oxide on capacitance performance of Zr-based metal organic framework electrodes", *J. Inorg. Organomet. Polym. Mater.*, 31 (2021) 1939-1984.

[13] M. Inagaki et al., **"Advanced Materials Science and Engineering of Carbon"**, Butterworth-Heinemann (2014).

[14] A.J. Kadhm and I.A. Abbas, "Influence of Copper and Zinc Doping on Optical Properties of Nano Nickel Oxide Films Deposited by Sol-Gel Method", *Nano Biomed. Eng.*, 14(4) (2022) 360-366.

[15] X. Guo et al., "Nanostructured graphene-based materials for flexible energy storage", *Ener.gy Stor. Mater.*, 9 (2017) 150-169.

[16] G. Kandhol et al., "Study of dielectric relaxation behavior of composites of Poly (vinyl alchohol) (PVA) and Reduced graphene oxide (RGO)", *Vacuum*, 160 (2019) 384-393.

[17] L.N. Ismail et al., "Optical Properties and Surface Morphology of (PMMA-TiO_2) Nanocomposites Thin films", *Adv. Mater. Res.*, 364 (2012) 105-109.
[18] M.E. El-Dahshan, **"Introduction to Material Science and Engineering"**, 2nd ed., King Saud Univ. Press (2002).
[19] S. Salman, N. Bakr and M.H. Mahmood, "Preparation and study of some optical properties of (PVA-Ni$(CH_3COO)_2$) composites", *Int. J. Curr. Res.*, 6(1) (2014) 9638-9643.
[20] N. Akram et al., "Influence of graphene oxide contents on mechanical behavior of polyurethane composites fabricated with different diisocyanates", *Polymers*, 13(3) (2021) 444.

